Oligomerization and Oxide Formation in Bismuth Aryl Alkoxides: Synthesis and Characterization of $Bi_4(\mu_4\text{-}O)(\mu\text{-}OC_6F_5)_6\{\mu_3\text{-}OBi(\mu\text{-}OC_6F_5)_3\}_2(C_6H_5CH_3)$, $Bi_8(\mu_4\text{-}O)_2(\mu_3\text{-}O)_2(\mu\text{-}OC_6F_5)_{16}$, $Bi_6(\mu_3\text{-}O)_4(\mu_3\text{-}OC_6F_5)\{\mu_3\text{-}OBi(OC_6F_5)_4\}_3$, $NaBi_4(\mu_3\text{-}O)_2(OC_6F_5)_9(THF)_2$, and $Na_2Bi_4(\mu_3\text{-}O)_2(OC_6F_5)_{10}(THF)_2$

Kenton H. Whitmire,* Silke Hoppe, Orson Sydora, Jennifer L. Jolas, and Carolyn M. Jones

Department of Chemistry, MS 60, Rice University, P.O. Box 1892, 6100 Main Street, Houston, Texas 77005-1892

Received April 20, 1999

Exposing $[Bi(OR)_3(toluene)]_2$ (**1**, R = OC_6F_5) to different solvents leads to the formation of larger polymetallic bismuth oxo alkoxides via ether elimination/oligomerization reactions. Three different compounds were obtained depending upon the conditions: $Bi_4(\mu_4\text{-}O)(\mu\text{-}OR)_6\{\mu_3\text{-}OBi(\mu\text{-}OR)_3\}_2(C_6H_5CH_3)$ (**2**), $Bi_8(\mu_4\text{-}O)_2(\mu_3\text{-}O)_2(\mu_2\text{-}OR)_{16}$ (**3**), $Bi_6(\mu_3\text{-}O)_4(\mu_3\text{-}OR)\{\mu_3\text{-}OBi(OR)_4\}_3$ (**4**). Compounds **2** and **3** can also be synthesized via an alcoholysis reaction between $BiPh_3$ and ROH in refluxing dichloromethane or chloroform. Related oxo complexes $NaBi_4(\mu_3\text{-}O)_2(OR)_9(THF)_2$ (**5**) and $Na_2Bi_4(\mu_3\text{-}O)_2(OR)_{10}(THF)_2$ (**6**) were obtained from $BiCl_3$ and NaOR in THF. The synthesis of **1** and $Bi(OC_6Cl_5)_3$ via salt elimination was successful when performed in toluene as solvent. For compounds **2**−**6** the single-crystal X-ray structures were determined. Variable-temperature NMR spectra are reported for **2**, **3**, and **5**.

Introduction

Homo- and heterometallic alkoxides have been studied as catalysts and as potential precursors for oxide-based ceramic materials as discussed in several reviews.[1−6] Bismuth oxide species are found in high T_c superconductors[2] as well as in catalysts,[3,5] oxide ion conductors,[4] and ceramic insulators and piezoelectric materials.[6,7] A number of bismuth alkoxides have been synthesized over the past decade as a means of preparing precursors for metal−organic chemical vapor deposition (MOCVD) or sol−gel syntheses of high-purity oxides. Hubert-Pfalzgraf and Buhro focused on the synthesis of bismuth alkoxides with increased volatility.[8,9] Studies of several fluorinated alkoxides of bismuth were published by our laboratory.[10−13]

An alkoxide must possess certain properties, both chemical and physical, to be useful as a precursor to oxide materials. These properties vary with the method employed for the alkoxide to oxide conversion. For instance, if the sol−gel process is used, an alkoxide precursor should be soluble, while for MOCVD the alkoxide precursors should be volatile. The complexes must decompose cleanly without leaving unwanted heteroatoms in the product oxide which often adversely affect the properties of the material.

The dimeric compound $[Bi(OR)_3(toluene)]_2$ (**1**) is reasonably stable under inert conditions and soluble in many organic solvents.[14] To better evaluate the properties of this compound as a potential precursor to oxide materials, its reactivity in solution was investigated. It was found that some solvents such as dichloromethane and chloroform promote the formation of larger polymetallic bismuth oxoalkoxides. In this paper we discuss the compounds $Bi_4(\mu_4\text{-}O)(\mu\text{-}OR)_6\{\mu_3\text{-}OBi(\mu\text{-}OR)_3\}_2(C_4H_8O)(C_6H_5CH_3)$ (**2**), $Bi_8(\mu_4\text{-}O)_2(\mu_3\text{-}O)_2(\mu\text{-}OR)_{16}$ (**3**), and $Bi_6(\mu_3\text{-}O)_4(\mu_3\text{-}OR)\{\mu_3\text{-}OBi(OR)_4\}_3$ (**4**), which were obtained upon dissolving **1** in various solvents, $NaBi_4(\mu_3\text{-}O)_2(OR)_9(THF)_2$ (**5**), and $Na_2Bi_4(\mu_3\text{-}O)_2(OR)_{10}(THF)_2$ (**6**), which was obtained from $BiCl_3$ and NaOR in THF (R = OC_6F_5) (Chart 1). Compounds **2**, **5**, and **6** were previously mentioned in a conference proceedings,[13] while a brief report of **4** has been published.[11]

Experimental Section

Synthetic Procedures. General Procedures. All reactions were carried out under an inert atmosphere of either argon or nitrogen using Schlenk, drybox, or high-vacuum techniques.[15] Solvents were freshly distilled from the appropriate drying agents prior to use: THF ($LiAlH_4$ followed by Na/Ph_2CO), diethyl ether ($LiAlH_4$ followed by Na/Ph_2CO), toluene (Na), CH_2Cl_2 (CaH_2), chloroform (alumina column), d_6-acetone (molecular sieves), and d_6-benzene, d_2-dichloromethane, and d_8-toluene (CaH_2). Ph_3BiBr_2[16,17] and **1**[12] were synthesized according to literature procedures. The phenols ROH and C_6Cl_5OH were sublimed

(1) Mehrotra, R. C.; Singh, A.; Sogani, S. *Chem. Rev.* **1994**, *94*, 1643.
(2) Page, C. J. H., C. S.; Burgoine, G. A. *Mater. Res. Soc. Symp. Proc.* **1992**, *271*, 155.
(3) Baidikova, I. V. V., V. P.; Mustafaev, N. M.; Mamedov, E. A.; Rizaev, R. G. *Kinet. Katal.* **1981**, *32*, 483.
(4) Bloom, I. H., M. C.; Zebrowski, J. P.; Myles, K. M.; Krumpelt, M. *Solid State Ionics* **1992**, *53*−*56*, 739.
(5) Ueda, W. T., J. M. *J. Chem. Soc., Chem. Commun.* **1988**, 1148.
(6) Hubert-Pfalzgraf, L. G. *New J. Chem.* **1987**, *11*, 663.
(7) Evans, A. G. *Mater. Sci. Eng.* **1985**, *71*, 3.
(8) Matchett, M. A.; Ciang, M. Y.; Buhro, W. E. *Inorg. Chem.* **1990**, *29*, 358.
(9) Massiani, M.-C.; Papiernik, R.; Hubert-Pfalzgraf, L. G.; Duran, J.-C. *Polyhedron* **1991**, *10*, 437.
(10) Jolas, J. L. H., S.; Whitmire, K. H. *Inorg. Chem.* **1997**, *36*, 3335.
(11) Jones, C. M. B., M. D.; Whitmire, K. H. *J. Chem. Soc., Chem. Commun.* **1992**, 1638.
(12) Jones, C. M. B., M. D.; Bachman, R. E.; Serra, D. L.; Hwu, S.-J.; Whitmire, K. H. *Inorg. Chem.* **1993**, *32*, 5136.
(13) Whitmire, K. H.; Jones, C. M.; Burkart, M. D.; Hutchison, J. C.; McKnight, A. L. In *Materials Research Society Proceedings: Better Ceramics Through Chemistry V*; Hampden-Smith, M. J., Klemperer, W. G., Brinker, C. J., Eds.; Materials Research Society: Pittsburgh, 1992; Vol. 271.
(14) Jones, C. M.; Burkart, M. D.; Whitmire, K. H. *Angew. Chem.* **1992**, *104*, 466; *Angew. Chem., Int. Ed. Engl.* **1992**, *31*, 451−452.
(15) Shriver, D. F. D., M. A. *The Manipulation of Air-Sensitive Compounds*; John Wiley and Sons: New York, 1986.

10.1021/ic990431m CCC: $19.00
Published on Web 12/18/1999

Chart 1

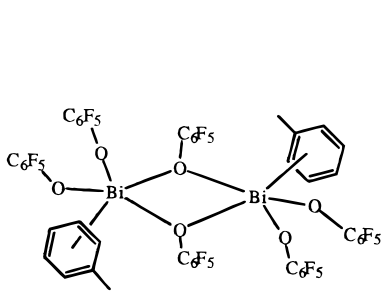

1

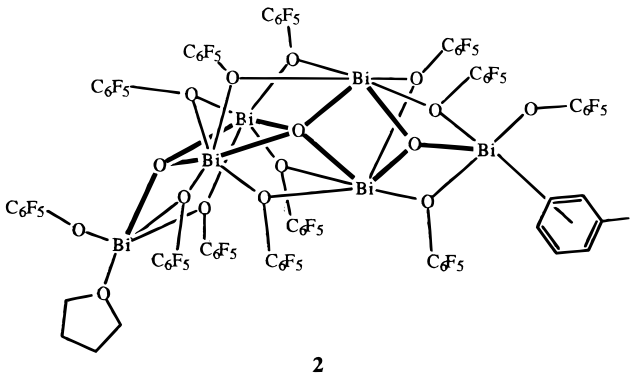

2

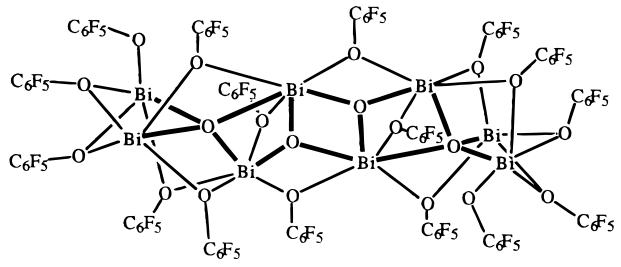

3

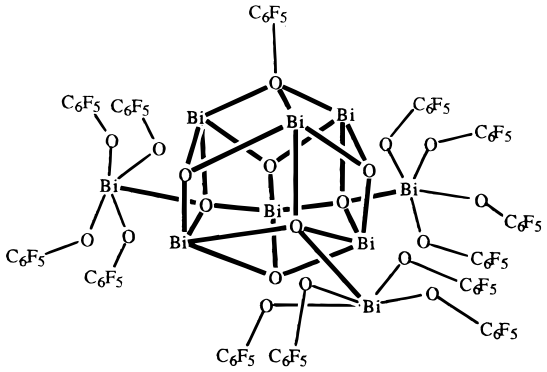

4

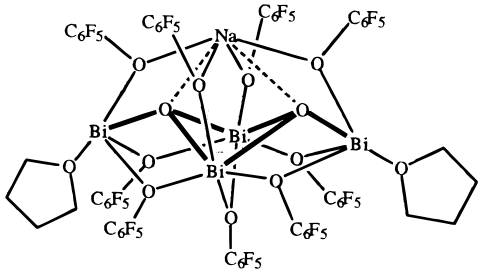

5

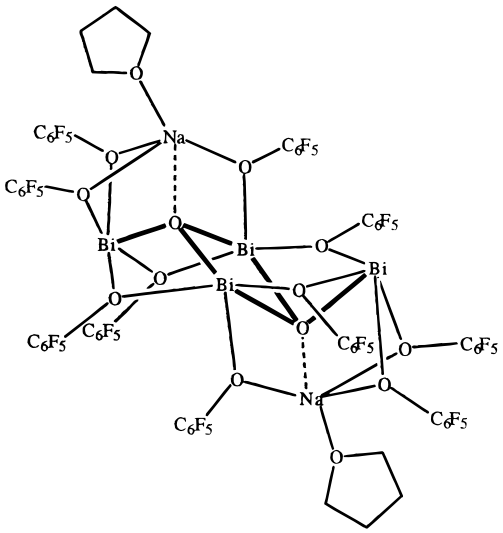

6

from molecular sieves under reduced pressure. $BiPh_3$ (Organometallics) was used as received. Sodium hydride (Aldrich), received as a mineral suspension, was washed with hexane and dried under vacuum.[15] NMR spectra were recorded on a Bruker AC250 (250 MHz ^1H, 235.34 MHz ^{19}F) spectrometer; chemical shifts are reported in parts per million on a scale relative to $CFCl_3$ (^{19}F NMR). Infrared spectra were taken on a Perkin-Elmer 1640 series spectrometer as KBr pellets. Elemental analyses were performed by Desert Analytics, Tucson, AZ (C, H, Cl, F, Bi), or by National Chemical Consulting, Tenafly, NJ (C, H, Cl, F, Br). Mass spectra were obtained on a Finnigan Mat 95. Table 1 summarizes the ^{19}F NMR data for compounds **2**, **3**, and **4**. Analyses of the byproducts of the reaction solutions by mass spectroscopy was accomplished by first transferring the residues under vacuum into a Schlenk container. Mass spectra of pentafluorophenol did not show any signs of production of bis(pentafluorophenyl) ether in the mass spectrum. The compounds turned out not to be volatile enough to obtain meaningful mass spectra.

Table 1. NMR Data for Compounds **2**, **3**, and **4** (ppm)[a]

		^{19}F NMR		
compd	solvent	*ortho*	*meta*	*para*
2	C_6D_6	−161.17, b	−162.54, b	−166.58, b
	CD_2Cl_2	−159.27, b	−161.99, b	−166.64, b
3	CD_2Cl_2	−161.21, d	−162.73, t	−168.19, t
4	C_6D_6	−162.89, d	−163.91, t	−169.57, s
	CD_2Cl_2	−160.78, s	−162.77, t	−169.79, s,b

[a] t = triplet, d = doublet, s = singlet, m = multiplet, b = broad.

(16) Michaelis, A.; Marquardt, A. *Liebigs Ann. Chem.* **1889**, *251*, 323−335.
(17) Michaelis, A.; Polis, A. *Ber. Dtsch. Chem. Ges.* **1887**, *20*, 55−56.

Table 2. Complete Crystallographic Data Collection and Structure Refinement Parameters for Compounds **2**, **3**, **4**, **5**, and **6**[a]

	2	**3**	**4**	**5**	**6**
empirical formula	$C_{91.30}H_{24.9}Bi_6F_{60}O_{16}$	$C_{99.37}H_{10.74}Bi_8Cl_{6.74}F_{80}O_{22}$	$C_{92}H_{16}Bi_9F_{65}O_{20}$	$C_{62}H_{16}Bi_4F_{45}NaO_{13}$	$C_{68}H_{16}Bi_4F_{50}Na_2O_{14}$
fw	3846.98	4987.03	5304.4	2682.66	2888.69
T (K)	193	193	193	223	193
cryst syst (space group)	triclinic ($P\bar{1}$)	triclinic ($P\bar{1}$)	triclinic ($P\bar{1}$)	monoclinic ($C2/c$)	monoclinic ($P2_1/c$)
a, Å	13.797(3)	14.292(3)	14.123(3)(3)	25.954(5)	12.008 (5)
b, Å	18.378(4)	15.111(3)	14.578(3)	14.755(3)	23.36(1)
c, Å	24.531(5)	17.545(4)	29.487(6)	19.916(4)	13.816(5)
α, deg	105.17(3)	112.19(3)	86.04(3)		
β, deg	104.82(3)	104.46(3)	81.79(3)	107.73(3)	92.71(3)
γ, deg	96.56(3	100.58(3)	61.98(3)		
λ(Mo Kα), Å	0.710 73	0.710 73	0.710 73	0.710 73	0.710 73
V, Å^3	5693.1(20)	3230.0(11)	5304.4(18)	7265(3)	3870(3)
Z	2	1	2	4	2
ρ_{calcd} g/cm^3	2.204	2.564	2.853	2.453	2.478
μ, mm^{-1}	9.397	11.175	15.054	9.844	9.231
goodness-of-fit, F^2	1.044	1.048	1.058	1.051	1.94
final R1 [$I > 2\sigma(I)$]	0.0516	0.0397	0.0764	0.0680	0.067
final wR2 [$I > 2\sigma(I)$]	0.1449	0.0931	0.2161	0.1415	0.069*

[a] $R_1 = \sum||F_o| - |F_c||/ - |F_o|$. $wR_2 = [\sum w(F_o^2 - F_c^2)^2]/\sum[w(F_o^2)^2]]^{0.5}$; $w = [\sigma^2(F_o^2) + (aP)^2 + bP]^{-1}$, where $P = (F_o^2 + 2F_c^2)/3$. [b] $w = 4F_o^2/\sigma^2(F_o^2)$, $p = 0.03$.

Synthesis of 2. Method 1. Compound **1** (0.3 g) was dissolved in 10 mL of freshly distilled dichloromethane. The clear yellow solution was stirred at room temperature for 5 min. Yellow solid **2** precipitated suddenly and was isolated by filtration. ^{19}F NMR spectroscopy confirmed the identity of the compound (see Table 1). Yield: 89%.

Method 2. $BiPh_3$ and 3 equiv ROH were dissolved in freshly distilled dichloromethane. The clear solution was stirred and heated to reflux for 2 days. Yellow solid **2** precipitated and was isolated by filtration. The powder was analyzed by ^{19}F NMR spectroscopy (see Table 1). Yield: 80%.

Method 3. Compound **1** was dissolved in THF and stirred for 6 h. After removal of the THF in vacuo the residue was dissolved in toluene and stirred for 2 h. Some yellow precipitate formed, which was removed by filtration through diatomaceous earth. Single crystals of **2** formed from the concentrated toluene filtrate at room temperature and were used to determine the crystal structure of **2.** Elemental analysis found (calcd for **2**·(THF)(toluene)$_3$: Bi, 32.31 (32.59); C, 30.8 (30.26); H, 0.99 (0.83). For unknown reasons the yield of conversion from **1** to **2** varies considerably using this method.

Synthesis of 3. Compound **1** was dissolved in freshly distilled dichloromethane, heated slightly to complete dissolution, filtered through diatomaceous earth, and layered with 1-hexene that had been purified by filtration through an alumina column. After one week of standing at room temperature, clear crystals of **4** formed together with pale yellow crystals of **3**. The crystals were separated manually under a microscope and used for single-crystal X-ray diffraction. Because of the formation of a mixture, it was not possible to obtain satisfactory analyses for **3**. Redissolving **3** in deuterated dichloromethane results in the formation of **4** in solution, so that it was impossible to record the NMR spectrum of pure **3**.

Synthesis of 4. Method 1. Compound **1** was dissolved in freshly distilled chloroform. A white precipitate formed rapidly. The solid was recrystallized from chloroform, yielding single crystals, which were not stable enough to collect a full X-ray data set; however, the partial structure solution clearly showed the metal−oxo core known from the structure determination of the product obtained from method 4. Consequently, redetermination of the structure was not pursued. The NMR spectra of freshly dissolved crystalline **4** contained signals due to pentafluorophenol and toluene. Elemental analysis found (calcd) for **4**·(ROH)$_2$(toluene): C, 24.03 (24.19); H; 0.17 (0.14); Bi, 39.93 (39.06); F, 30.53 (29.60).

Method 2. Compound **1** was dissolved in freshly distilled dichloromethane with heating. The warm solution was filtered through diatomaceous earth, and the filtrate was layered with 1-hexene. The 1-hexene had been purified by passing it through an alumina column. Colorless single crystals of **4** formed at room temperature together with crystals of **3**.

Method 3. Compound **1** was dissolved in freshly distilled toluene. The yellow solution was exposed to oxygen and moisture by evacuating the flask and filling it with air. White solid precipitated after 10 min from the yellow solution. The NMR spectrum confirmed the identity of the product (see Table 1).

Method 4. Compound **1** was dissolved in freshly distilled toluene. The toluene solution was purged with argon gas which was saturated with water, resulting in the formation of **4** as confirmed by NMR. Single crystals were obtained upon exposing a toluene solution of **1** to air and allowing it to stand for several days.

Synthesis of 5 and 6. A THF solution of ROH (2.30 g, 12.5 mmol, in 50 mL) was added to a slurry of NaH in THF (2.75 g, 115 mmol, in 30 mL), stirred for 1 h, and filtered through diatomaceous earth. The filtrate was added to a solution of $BiCl_3$ in THF (1.50 g, 4.75 mmol, in 50 mL) via cannula. A yellow solution resulted which contained a fine white precipitate. After the mixture was stirred for 2 h, the solvent was removed in vacuo. This resulted in a yellow oil, which was extracted into 75 mL of toluene. After filtration through diatomaceous earth, the solvent was reduced to approximately 25 mL. Large, pale yellow monoclinic-shaped crystals formed upon standing and were collected by filtration. Yield: 46% based on Bi. The side product ROR was identified by mass spectrometry of the reaction mixture in THF ($M^+ = 350$). Elemental analysis found (calcd): Bi, 30.83 (31.16); Na, 1.12 (0.86). In some syntheses of **5**, **6** was obtained as pale yellow crystals, but it proved difficult to obtain reproducibly. Consequently, elemental analyses of **6** are not available.

Synthesis of $Bi(OC_6Cl_5)_3$. Freshly prepared $NaOC_6Cl_5$ (3 mmol) was dissolved in toluene. Solid $BiCl_3$ (1 mmol) was added to this solution. The reaction mixture was stirred for 24 h, filtered, and cooled to −10 °C. The resulting yellow precipitate was filtered from the solution, dried, and analyzed. Elemental analysis found (calcd): Cl, 53.49 (52.92); Bi, 19.94 (20.79); C, 21.88 (21.52); H, 0.56.

Single-Crystal X-ray Diffraction. Crystal data and data collection and refinement parameters are given in Table 2. Crystals were examined under mineral oil, and the ones selected for data collection were glued to the tip of a glass fiber and transferred to a cold nitrogen stream of a Rigaku AFC5S four-circle diffractometer with the Texsan 5.0 software package using Mo Kα radiation ($\lambda = 0.710\ 73$ Å).[18] The data were corrected for Lorentz and polarization factors and for absorption using ψ-scans. The stabilities of the crystals and the X-ray beam were monitored by measuring three standard reflections at a frequency of every 150 observations. The analytical form of the scattering factors for the appropriate neutral atoms were corrected for both the real ($\Delta f'$)

(18) TEXSAN v. 5.0, Single-Crystal Structure Analysis Software, Molecular Structure Co., 1990.

Table 3. Selected Bond Lengths (Å) and Angles (deg) for **2**

			Distances				
Bi(1)−O(1)	2.098(12)	Bi(1)−O(100)	2.118(12)	Bi(4)−O(80)	2.262(11)	Bi(4)−O(2)	2.323(11)
Bi(1)−O(10)	2.278(11)	Bi(1)−O(20)	2.343(11)	Bi(4)−O(70)	2.419(10)	Bi(4)−O(50)	2.496(10)
Bi(2)−O(1)	2.164(11)	Bi(2)−O(2)	2.250(12)	Bi(4)−O(90)	2.509(11)	Bi(4)−Bi(5)	3.3718(13)
Bi(2)−O(30)	2.277(11)	Bi(2)−O(60)	2.404(10)	Bi(5)−O(3)	2.151(11)	Bi(5)−O(2)	2.291(11)
Bi(2)−O(20)	2.555(11)	Bi(2)−O(80)	2.622(11)	Bi(5)−O(70)	2.312(11)	Bi(5)−O(60)	2.358(11)
Bi(2)−Bi(3)	3.3900(14)	Bi(3)−O(1)	2.195(12)	Bi(5)−O(120)	2.492(11)	Bi(5)−O(40)	2.652(11)
Bi(3)−O(2)	2.224(11)	Bi(3)−O(40)	2.234(11)	Bi(6)−O(110)	2.108(12)	Bi(6)−O(3)	2.131(12)
Bi(3)−O(50)	2.383(11)	Bi(3)−O(30)	2.468(11)	Bi(6)−O(120)	2.266(11)	Bi(6)−O(90)	2.386(11)
Bi(3)−O(10)	2.631(12)	Bi(4)−O(3)	2.180(13)	Bi(6)−O(135)	2.629(14)		
			Angles				
O(1)−Bi(1)−O(100)	96.2(5)	O(1)−Bi(1)−O(10)	70.8(4)	O(60)−Bi(5)−O(120)	89.2(4)	O(3)−Bi(5)−O(40)	130.8(4)
O(100)−Bi(1)−O(10)	83.4(5)	O(1)−Bi(1)−O(20)	72.4(4)	O(2)−Bi(5)−O(40)	65.2(4)	O(70)−Bi(5)−O(40)	80.5(4)
O(100)−Bi(1)−O(20)	79.7(4)	O(10)−Bi(1)−O(20)	137.3(4)	O(60)−Bi(5)−O(40)	101.7(4)	O(120)−Bi(5)−O(40)	161.8(4)
O(1)−Bi(2)−O(2)	68.5(4)	O(1)−Bi(2)−O(30)	70.8(4)	O(110)−Bi(6)−O(3)	94.0(5)	O(110)−Bi(6)−O(120)	83.6(5)
O(2)−Bi(2)−O(30)	74.0(4)	O(1)−Bi(2)−O(60)	79.9(4)	O(3)−Bi(6)−O(120)	69.7(4)	O(110)−Bi(6)−O(90)	84.5(5)
O(2)−Bi(2)−O(60)	70.4(4)	O(30)−Bi(2)−O(60)	140.1(4)	O(3)−Bi(6)−O(90)	67.7(4)	O(120)−Bi(6)−O(90)	134.6(4)
O(1)−Bi(2)−O(20)	67.2(4)	O(2)−Bi(2)−O(20)	135.6(4)	O(110)−Bi(6)−O(135)	76.2(5)	O(3)−Bi(6)−O(135)	146.8(4)
O(30)−Bi(2)−O(20)	93.2(4)	O(60)−Bi(2)−O(20)	99.8(4)	O(120)−Bi(6)−O(135)	77.7(4)	O(90)−Bi(6)−O(135)	140.3(4)
O(1)−Bi(2)−O(80)	130.7(4)	O(2)−Bi(2)−O(80)	67.4(4)	O(80)−Bi(4)−O(2)	72.9(4)	O(3)−Bi(4)−O(70)	68.2(4)
O(30)−Bi(2)−O(80)	76.9(4)	O(60)−Bi(2)−O(80)	104.6(4)	O(80)−Bi(4)−O(70)	142.2(4)	O(2)−Bi(4)−O(70)	73.6(4)
O(20)−Bi(2)−O(80)	151.8(3)	O(1)−Bi(3)−O(2)	68.4(4)	Bi(3)−O(2)−Bi(5)	117.1(5)	Bi(2)−O(2)−Bi(5)	113.3(5)
O(1)−Bi(3)−O(40)	84.7(4)	O(2)−Bi(3)−O(40)	73.9(4)	Bi(3)−O(2)−Bi(4)	120.2(5)	Bi(2)−O(2)−Bi(4)	115.0(5)
O(1)−Bi(3)−O(50)	132.9(4)	O(2)−Bi(3)−O(50)	67.6(4)	Bi(5)−O(2)−Bi(4)	93.9(4)	Bi(6)−O(3)−Bi(5)	120.2(5)
O(40)−Bi(3)−O(50)	98.7(4)	O(1)−Bi(3)−O(30)	66.7(4)	Bi(6)−O(3)−Bi(4)	122.7(6)	Bi(5)−O(3)−Bi(4)	102.2(5)
O(2)−Bi(3)−O(30)	70.8(4)	O(40)−Bi(3)−O(30)	140.7(4)	C(11)−O(10)−Bi(1)	133.3(6)	C(11)−O(10)−Bi(3)	123.9(7)
O(50)−Bi(3)−O(30)	83.6(4)	O(1)−Bi(3)−O(10)	62.7(4)	Bi(1)−O(10)−Bi(3)	99.9(4)	C(31)−O(30)−Bi(2)	131.5(8)
O(2)−Bi(3)−O(10)	129.2(4)	O(40)−Bi(3)−O(10)	88.3(4)	C(31)−O(30)−Bi(3)	131.5(8)	Bi(2)−O(30)−Bi(3)	91.1(3)
O(50)−Bi(3)−O(10)	163.1(3)	O(30)−Bi(3)−O(10)	100.7(4)	C(41)−O(40)−Bi(3)	124.6(7)	C(41)−O(40)−Bi(5)	128.6(8)
O(3)−Bi(4)−O(80)	83.6(4)	O(3)−Bi(4)−O(2)	68.4(4)	Bi(3)−O(40)−Bi(5)	103.7(4)	C(51)−O(50)−Bi(3)	124.2(6)
O(80)−Bi(4)−O(2)	72.9(4)	O(3)−Bi(4)−O(70)	68.2(4)	C(51)−O(50)−Bi(4)	128.1(6)	Bi(3)−O(50)−Bi(4)	107.8(4)
O(80)−Bi(4)−O(70)	142.2(4)	O(2)−Bi(4)−O(70)	73.6(4)	C(61)−O(60)−Bi(5)	123.2(7)	C(61)−O(60)−Bi(2)	129.2(7)
O(3)−Bi(4)−O(50)	128.0(4)	O(80)−Bi(4)−O(50)	101.7(4)	Bi(5)−O(60)−Bi(2)	105.6(4)	C(71)−O(70)−Bi(5)	130.6(8)
O(2)−Bi(4)−O(50)	64.3(4)	O(70)−Bi(4)−O(50)	78.6(4)	C(71)−O(70)−Bi(4)	129.0(8)	Bi(5)−O(70)−Bi(4)	90.9(3)
O(3)−Bi(4)−O(90)	64.7(4)	O(80)−Bi(4)−O(90)	87.7(4)	C(81)−O(80)−Bi(4)	121.1(7)	C(81)−O(80)−Bi(2)	133.0(8)
O(2)−Bi(4)−O(90)	130.8(4)	O(70)−Bi(4)−O(90)	101.5(4)	Bi(4)−O(80)−Bi(2)	104.0(4)	C(91)−O(90)−Bi(6)	134.2(7)
O(50)−Bi(4)−O(90)	164.6(4)	O(3)−Bi(5)−O(2)	69.5(4)	C(91)−O(90)−Bi(4)	124.7(7)	Bi(6)−O(90)−Bi(4)	101.2(4)
O(3)−Bi(5)−O(70)	70.8(4)	O(2)−Bi(5)−O(70)	76.2(4)	C(101)−O(100)−Bi(1)	125.8(8)	C(111)−O(110)−Bi(6)	121.6(8)
O(3)−Bi(5)−O(60)	80.0(4)	O(2)−Bi(5)−O(60)	70.6(4)	C(121)−O(120)−Bi(6)	135.6(7)	C(121)−O(120)−Bi(5)	121.7(7)
O(70)−Bi(5)−O(60)	141.7(4)	O(3)−Bi(5)−O(120)	65.1(4)	Bi(6)−O(120)−Bi(5)	102.5(4)	C(134)−O(135)−Bi(6)	127.6(13)
O(2)−Bi(5)−O(120)	132.8(4)	O(70)−Bi(5)−O(120)	100.0(4)	C(131)−O(135)−Bi(6)	124.9(14)		

and the imaginary ($\Delta f''$) components of anomalous dispersion.[19] All structures except for that of **6** were solved with direct methods or Patterson synthesis using the Siemens Package SHELXTL-PLUS 5.0 for PC, and a full matrix least-squares refinement on F^2 was performed using SHELXL-93.[20,21] Compound **6** was solved using the direct methods routine in the TEXSAN software package.[18] Where appropriate, hydrogen atoms were included in calculated positions using the riding model tied to the carbon atom to which they are bound.

Structure of 2. Yellow crystals of **2**·1.3C_7H_8 suitable for X-ray diffraction were grown by cooling a concentrated toluene solution of the compound to −10 °C. Direct methods located the six bismuth atoms, and the other non-hydrogen atoms were located by successive Fourier difference maps. A thermal ellipsoid plot of the molecule is provided in Figure 1. All non-hydrogen atoms were refined anisotropically. The OR ligands of **2** were refined as rigid groups restrained to fit local C_{2v} symmetry (C_2 axis along the O−C1−C4 vector). The fluorine and alkoxide oxygen atoms were refined with a common distance to each of the ring carbons *ortho* to their position. In addition to the pentafluorophenoxide ligands, one Bi(6) is ligated by a THF molecule and Bi(1) is coordinated to a toluene ring. In the latter case, the methyl group of the toluene is disordered, having one major component which was refined at 0.5 occupancy. The other components appear to be spread out over the rest of the ring and were not included in the refinement. Additionally, there are four other toluene locations in the crystal lattice. Two of these molecules were refined at half-occupancy in general positions, and the other two were situated about inversion centers and were refined at 0.3 occupancy, giving a total of 1.3 lattice solvent toluene molecules per cluster. There is some indication that lattice solvent molecules of this type are in reality present at full occupancy but disordered in the cavity in which they sit.[22] If full occupancy is considered, then the formula of this compound becomes $Bi_4(\mu_4\text{-O})(\mu\text{-OR})_6\{\mu_3\text{-OBi}(\mu\text{-OR})_3\}_2(C_6H_5CH_3)\cdot 3(C_6H_5CH_3)$. Selected data collection and refinement parameters can be found in Table 2. A complete list of bond distances, bond angles, anisotropic displacement parameters, and hydrogen atom coordinates is given in the Supporting Information. Selected bond distances and angles are provided in Table 3.

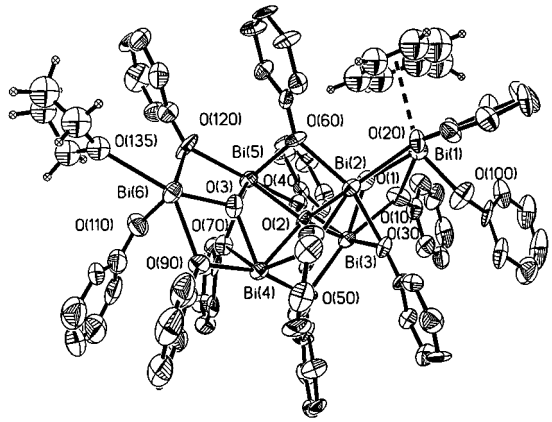

Figure 1. Thermal ellipsoid plot of **2**·1.3$C_6H_5CH_3$. The 50% probability level was chosen for clarity. Fluorine atoms have been omitted.

(19) *International Tables of X-ray Crystallography*; Kynoch Press: Birmingham, 1974.
(20) Sheldrick, G. M. SHELXL-93, Gottingen, Germany, 1993.
(21) Sheldrick, G. M. SHELXTL PLUS PC 5.0, Siemens Crystallographic Research Systems, Madison, WI, 1995.
(22) Rheingold, A. L. Personal communication.

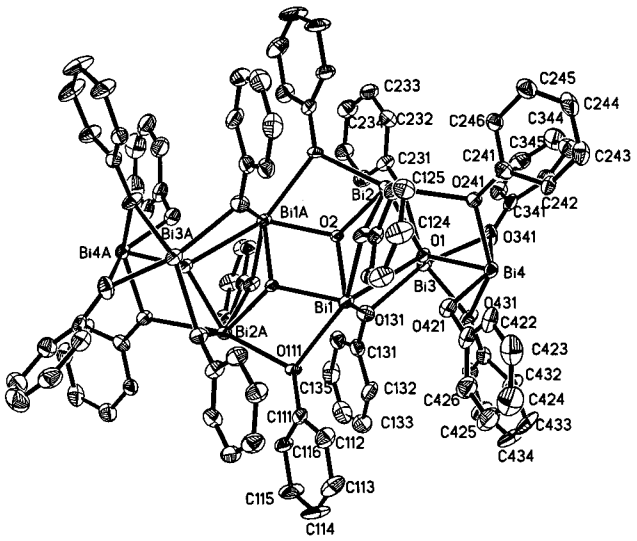

Figure 2. Thermal ellipsoid plot of **3** at the 50% probability level. Fluorine atoms have been omitted.

Structure of 3. Yellow crystals of **3** suitable for X-ray diffraction were grown by storing a concentrated dichloromethane solution of **1** layered with 1-hexene at room temperature. As with **2**, the eight bismuth atoms were located in the initial direct methods solution, and the non-hydrogen atoms were located in successive Fourier difference maps. A thermal ellipsoid plot of **3** is given in Figure 2. All non-hydrogen atoms were refined anisotropically. Dichloromethane solvent molecules were found in the lattice and determined to be disordered. One CH_2Cl_2 was modeled over two sites with partial occupancies which were determined using free variables. The total occupancy of the molecule was 80%, with 50% in one and 30% in the other orientation. After these values were determined, the occupancy of those two solvents was fixed and not further refined. The second CH_2Cl_2 with a partial occupancy of 89% also showed slight positional disorder which was not resolved. A second free variable was used to refine all C−Cl distances to the same value. All non-hydrogen atoms except those of the lattice solvents were refined anisotropically. The largest peak in the final difference map was located near the chlorine of the disordered solvent molecule (1.727 e/Å^3). Selected data collection and refinement parameters can be found in Table 2. Selected bond distances and angles are provided in Table 4.

Structure of 4. A preliminary account of the X-ray structure analyses for **4**·$(THF)_2$ and **4**·$(toluene)_2$ was published.[11] Single crystals of **4** were obtained using method 2 but were of insufficient quality for a full refinement of the parameters of the lighter atoms due to the decay of the crystals in the X-ray beam. The cell constants found were a = 14.65 Å, b = 15.61 Å, c = 26.62 Å, α = 79.50°, β = 79.48°, γ = 72.02°, and V = 5641 Å^3. Recrystallization of this compound from dichloromethane and chloroform solutions did result in crystals that were more stable in the X-ray beam. From a reasonable refinement of the Bi_9O_7 core for these partial data sets, we were able to conclude that the compound produced from method 2 was essentially the same as that obtained from method 4 but with differing amounts and/or arrangements of lattice solvent molecules. Single crystals of **4**·$2C_7H_8$ grown from toluene solution proved suitable for a single-crystal X-ray analysis, but these also showed some decay during data collection (ca. 5%). The structure was solved using direct methods which located the bismuth atoms. The remaining atoms were located by successive electron density difference maps. The bismuth and fluorine atoms only were refined anisotropically with mild restraints applied to the fluorine atom anisotropic displacement parameters. The two toluene solvent molecules were refined as rigid groups. A thermal ellipsoid plot is presented in Figure 3. Selected data collection and refinement parameters can be found in Table 2 with selected bond distances and angles provided in Table 5.

Structure of 5. Yellow crystals of **5** suitable for X-ray diffraction were grown by cooling a concentrated toluene solution to −10 °C. Systematic absences indicated the possibility of space groups *Cc* and *C*2/*c*. The main problem in choosing *C*2/*c* is that one OC_6F_5 group sits close to but not exactly on the crystallographic C_2 axis. This problematic disorder suggested that the proper solution might be in *Cc*, which does not have the C_2 axis. Attempted structure solution in *Cc*, however, would not allow location of all the phenyl rings. A second data set including Freidels pairs was collected to facilitate distinguishing between the centric and acentric cell, and a further attempt at modeling the compound in *Cc* was carried out by constructing the entire molecule in *C*2/*c* and then transforming the symmetry operations to those appropriate for *Cc* and using the complete data set including Friedel pairs. Isotropic refinement with a strong damping restraint yielded reasonable residuals; however, attempts to refine the F and O atoms anisotropically were not successful. The refinement in *C*2/*c* was, therefore, chosen as the best solution. The sodium, bismuth, and μ_3-oxygen atoms were refined anisotropically. The OR ligands were refined as rigid groups as described for **2**. The phenyl ring of the bridging alkoxide ligand between Bi(1) and Bi(1A) was located about 7° off

Table 4. Selected Bond Lengths (Å) and Angles (deg) for **3**

			Distances				
Bi(1)−O(1)	2.730(8)	Bi(1)−O(2)	2.193(7)	Bi(3)−O(1)	2.108(8)	Bi(3)−O(131)	2.433(9)
Bi(1)−O(2)#1	2.182(7)	Bi(1)−O(131)	2.316(8)	Bi(3)−O(231)	2.356(8)	Bi(3)−O(341)	2.220(9)
Bi(1)−O(111)	2.525(8)	Bi(1)−O(121)	2.476(8)	Bi(3)−O(431)	2.312(8)	Bi(4)−O(1)	2.135(7)
Bi(2)−O(1)	2.335(7)	Bi(2)−O(2)	2.139(7)	Bi(4)−O(421)	2.158(9)	Bi(4)−O(241)	2.233(8)
Bi(2)−O(111)#1	2.333(8)	Bi(2)−O(121)	2.337(8)	Bi(4)−O(431)	2.416(8)	Bi(4)−O(341)	2.595(9)
Bi(2)−O(231)	2.360(8)	Bi(2)−O(241)	2.703(8)				
			Angles				
O(2)#1−Bi(1)−O(2)	71.9(3)	O(2)#1−Bi(1)−O(131)	105.9(3)	O(341)−Bi(3)−O(231)	80.5(3)	O(431)−Bi(3)−O(231)	138.0(3)
O(2)−Bi(1)−O(131)	75.7(3)	O(2)#1−Bi(1)−O(121)	90.8(3)	O(1)−Bi(3)−O(131)	75.7(3)	O(341)−Bi(3)−O(131)	145.3(3)
O(2)−Bi(1)−O(121)	67.4(3)	O(131)−Bi(1)−O(121)	132.1(3)	O(431)−Bi(3)−O(131)	81.1(3)	O(231)−Bi(3)−O(131)	110.0(3)
O(2)#1−Bi(1)−O(111)	65.2(3)	O(2)−Bi(1)−O(111)	124.4(3)	O(1)−Bi(4)−O(421)	77.6(3)	O(1)−Bi(4)−O(241)	74.7(3)
O(131)−Bi(1)−O(111)	83.6(3)	O(121)−Bi(1)−O(111)	142.8(3)	O(421)−Bi(4)−O(241)	93.9(3)	O(1)−Bi(4)−O(431)	68.2(3)
O(2)#1−Bi(1)−O(1)	133.7(2)	O(2)−Bi(1)−O(1)	61.8(2)	O(421)−Bi(4)−O(431)	93.0(3)	O(241)−Bi(4)−O(431)	139.7(3)
O(131)−Bi(1)−O(1)	66.8(3)	O(121)−Bi(1)−O(1)	69.3(2)	O(1)−Bi(4)−O(341)	67.9(3)	O(421)−Bi(4)−O(341)	143.2(3)
O(111)−Bi(1)−O(1)	147.7(3)	O(2)−Bi(2)−O(111)#1	69.4(3)	O(241)−Bi(4)−O(341)	89.1(3)	O(431)−Bi(4)−O(341)	63.0(3)
O(2)−Bi(2)−O(1)	70.0(3)	O(111)#1−Bi(2)−O(1)	137.4(3)	Bi(3)−O(1)−Bi(4)	107.9(3)	Bi(3)−O(1)−Bi(2)	112.1(3)
O(2)−Bi(2)−O(121)	70.9(3)	O(111)#1−Bi(2)−O(121)	99.5(3)	Bi(4)−O(1)−Bi(2)	119.7(3)	Bi(3)−O(1)−Bi(1)	106.2(3)
O(1)−Bi(2)−O(121)	78.9(3)	O(2)−Bi(2)−O(231)	78.4(3)	Bi(4)−O(1)−Bi(1)	121.4(3)	Bi(2)−O(1)−Bi(1)	88.2(2)
O(111)#1−Bi(2)−O(231)	90.4(3)	O(1)−Bi(2)−O(231)	69.3(3)	Bi(2)−O(2)−Bi(1)#1	120.5(3)	Bi(2)−O(2)−Bi(1)	109.4(3)
O(121)−Bi(2)−O(231)	141.7(3)	O(2)−Bi(2)−O(241)	129.9(3)	Bi(1)#1−O(2)−Bi(1)	108.1(3)	Bi(2)#1−O(111)−Bi(1)	101.0(3)
O(111)#1−Bi(2)−O(241)	159.6(3)	O(1)−Bi(2)−O(241)	63.0(2)	Bi(2)−O(121)−Bi(1)	94.5(3)	Bi(1)−O(131)−Bi(3)	109.8(3)
O(121)−Bi(2)−O(241)	83.9(3)	O(231)−Bi(2)−O(241)	99.4(3)	Bi(3)−O(231)−Bi(2)	102.9(3)	Bi(4)−O(241)−Bi(2)	102.7(3)
O(1)−Bi(3)−O(341)	76.1(3)	O(1)−Bi(3)−O(431)	70.7(3)	Bi(3)−O(341)−Bi(4)	90.5(3)	Bi(3)−O(431)−Bi(4)	93.0(3)
O(341)−Bi(3)−O(431)	70.7(3)	O(1)−Bi(3)−O(231)	73.2(3)				

[a] Symmetry transformations used to generate equivalent atoms: (#1) $-x+3, -y+3, -z+1$.

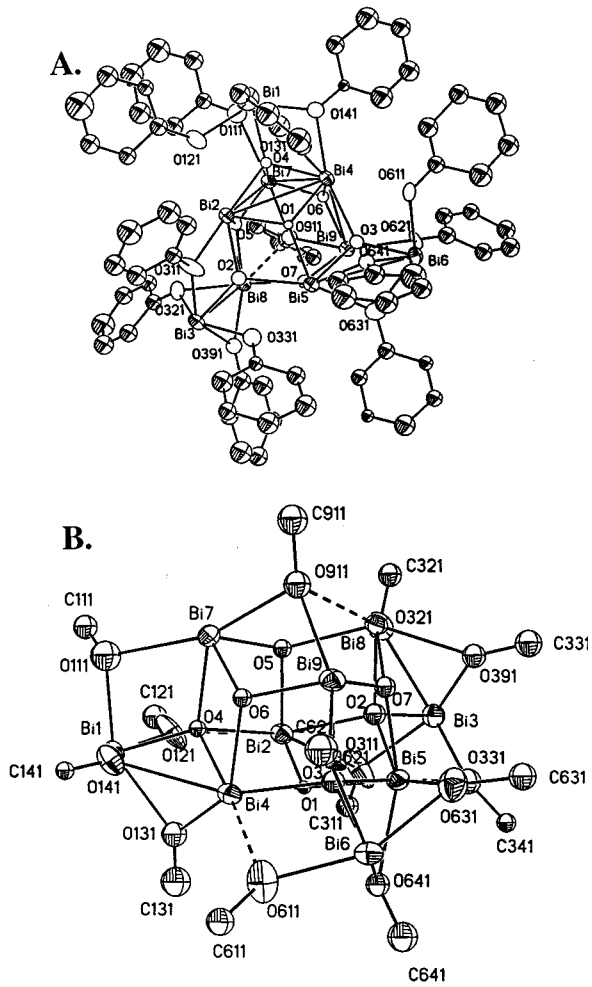

Figure 3. (A) Thermal ellipsoid plot of **4** at the 50% probability level. Fluorine atoms have been omitted. (B) Thermal ellipsoid plot of the core of **4** with all but the ipso-carbon atoms of the C_6F_5 rings omitted for clarity.

the symmetry axis and was refined as a single ring with half-occupancy. The structure of the molecule is shown in Figure 4, while Figure 5 shows the Na^+ ion enviroment. Selected data collection and refinement parameters can be found in Table 2. Selected bond distances and angles are provided in Table 6.

Structure of 6. Pale yellow blocklike crystals of **6** suitable for single-crystal X-ray diffraction were grown from a toluene extract of the reaction solution. The structure was solved using direct methods which located the bismuth atoms. The remaining atoms were located by successive electron density difference maps. Due to the limitation of the number of observed data, only the Bi and Na atoms were refined anisotropically. A thermal ellipsoid plot of **6** is provided in Figure 6. Figure 7 shows the Na^+ ion environment. Selected bond distances and angles are provided in Table 7.

Results and Discussion

Syntheses. By dissolving the bismuth pentafluorophenoxide dimer **1** in different solvents under various conditions, a number of bismuth oxo alkoxide compounds are obtained. Scheme 1 summarizes these transformations. The toluene ligands of **1** are weakly coordinated and are easily displaced by coordinating solvents such as THF.[12]

The metathesis reaction between $BiCl_3$ and NaOR was originally carried out in THF with the intent of forming $Bi(OR)_3$. However, when this methodology was employed, regardless of the care taken, products containing oxide ligands and/or Na^+ ions were isolated, and we were never able to isolate $Bi(OR)_3$ or its dimer form **1** by that method. The characterization of **7** showed that the dimer was not inherently unstable toward

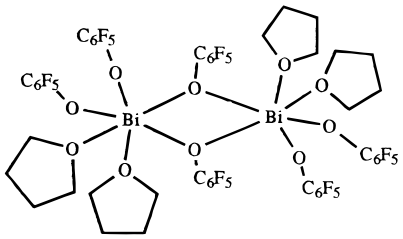

7

THF.[14] Alcoholysis of $BiPh_3$, however, did prove useful for synthesizing **1**, and this discovery has allowed exploration of its reaction chemistry.[12] The salt metathesis reaction when performed in toluene, however, was found to yield **1**. Surprisingly, we were able to produce $Bi(OC_6Cl_5)_3$ (as determined by elemental analyses) from $NaOC_6Cl_5$ and $BiCl_3$ in toluene, but the alcoholysis method employing $BiPh_3$ and HOC_6Cl_5 was not successful. Since no routine spectroscopic handle is available for characterizing $Bi(OC_6Cl_5)_3$ and single crystals could not be grown, we do not yet know if this compound exists as a monomer or oligomer in the solid state. It is interesting to note in Scheme 1 that a number of the compounds may be built of the unit $Bi_2O(OR)_4$, which can be thought to arise from **1** by the elimination of ROR. Thus, **2** is $[Bi_2O(OR)_4]_3$, **3** is $[Bi_2O(OR)_4]_4$, **5** is $[Bi_2O(OR)_4]_2 \cdot NaOR \cdot 2THF$, and **6** is $[Bi_2O(OR)_4]_2 \cdot 2NaOR \cdot 2THF$. While the conversion of **5** to **6** by simple addition of NaOR is obvious, we have not been able to accomplish this directly because the addition of NaOR to **5** turns out to be exceedingly difficult to control and has led to other compounds in all attempts to date. From these empirical observations, we have concluded that bismuth-bound OR ligands are very susceptible to attack at the *ipso* carbon of the phenyl ring, resulting in ether elimination. Note that the conversion of **2** to **3** does not require further oxide ligand formation or hydrolysis since both are built up of the same simple building block **12**, and that interconversion may be accomplished by a solution equilibration of the units.

Solvent choice is very important in determining the nature of the products obtained. Compound **1** dissolves in toluene to form a monomeric $Bi(OR)_3$ complex, most likely in a more highly solvated form.[12] Compound **2** is obtained by dissolving **1** in dichloromethane, in THF, or in THF with *traces* of NaOR. Addition of NaOR to the THF solution of **1** does not appear to change the course of the reaction; however, it does expedite product formation. Using more than 1/10 equiv of NaOR per bismuth atom, however, yields a mixture of products containing **2** and other sodium bismuth oxo alkoxides.[10] Note that for a reaction between **1** and NaOR in a carefully controlled ratio of 1:2 the adduct $NaBi(OR)_4$ (**8**) is formed; the same reaction with a **1**:NaOR ratio of 1:4 yields $Na_4Bi_2O(OR)_8(THF)_4$ (**9**) and

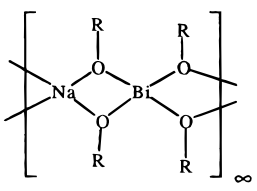

8

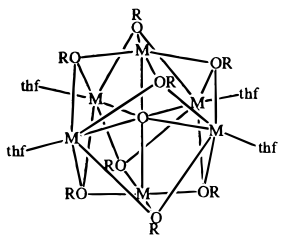

9

Table 5. Selected Bond Lengths (Å) and Angles (deg) for **4**

Distances							
Bi(1)−O(4)	2.096(17)	Bi(1)−O(121)	2.25(2)	Bi(5)−O(631)	2.48(2)	Bi(5)−O(641)	2.52(2)
Bi(1)−O(111)	2.26(2)	Bi(1)−O(141)	2.30(2)	Bi(5)−O(2)	2.551(19)	Bi(6)−O(3)	2.135(19)
Bi(1)−O(131)	2.35(2)	Bi(2)−O(1)	2.173(16)	Bi(6)−O(611)	2.23(2)	Bi(6)−O(621)	2.313(19)
Bi(2)−O(2)	2.229(19)	Bi(2)−O(5)	2.229(18)	Bi(6)−O(641)	2.339(19)	Bi(6)−O(631)	2.43(2)
Bi(2)−O(4)	2.450(16)	Bi(2)−O(311)	2.61(2)	Bi(7)−O(5)	2.132(17)	Bi(7)−O(6)	2.179(18)
Bi(3)−O(2)	2.154(18)	Bi(3)−O(331)	2.17(2)	Bi(7)−O(4)	2.260(17)	Bi(7)−O(911)	2.44(2)
Bi(3)−O(311)	2.26(2)	Bi(3)−O(391)	2.36(2)	Bi(7)−O(111)	2.69(2)	Bi(8)−O(5)	2.199(18)
Bi(3)−O(321)	2.53(2)	Bi(4)−O(1)	2.171(15)	Bi(8)−O(2)	2.23(2)	Bi(8)−O(7)	2.267(18)
Bi(4)−O(6)	2.233(18)	Bi(4)−O(4)	2.300(17)	Bi(8)−O(321)	2.38(2)	Bi(8)−O(391)	2.47(2)
Bi(4)−O(3)	2.453(19)	Bi(4)−O(131)	2.52(2)	Bi(9)−O(7)	2.117(18)	Bi(9)−O(6)	2.120(17)
Bi(4)−O(141)	2.63(2)	Bi(5)−O(7)	2.160(19)	Bi(9)−O(3)	2.218(19)	Bi(9)−O(621)	2.511(18)
Bi(5)−O(1)	2.191(16)	Bi(5)−O(3)	2.294(18)	Bi(9)−O(911)	2.57(2)		
Angles							
O(4)−Bi(1)−O(121)	73.0(7)	O(4)−Bi(1)−O(111)	75.7(8)	O(3)−Bi(6)−O(631)	65.8(7)	O(611)−Bi(6)−O(631)	141.3(8)
O(121)−Bi(1)−O(111)	85.1(9)	O(4)−Bi(1)−O(141)	69.5(7)	O(621)−Bi(6)−O(631)	87.7(7)	O(641)−Bi(6)−O(631)	75.4(7)
O(121)−Bi(1)−O(141)	142.5(8)	O(111)−Bi(1)−O(141)	86.5(8)	O(5)−Bi(7)−O(6)	97.0(7)	O(5)−Bi(7)−O(4)	76.1(6)
O(4)−Bi(1)−O(131)	68.7(7)	O(121)−Bi(1)−O(131)	89.4(9)	O(6)−Bi(7)−O(4)	73.5(6)	O(5)−Bi(7)−O(911)	75.3(7)
O(111)−Bi(1)−O(131)	144.0(8)	O(141)−Bi(1)−O(131)	76.6(8)	O(6)−Bi(7)−O(911)	72.2(7)	O(4)−Bi(7)−O(911)	131.5(7)
O(1)−Bi(2)−O(2)	74.1(7)	O(1)−Bi(2)−O(5)	97.4(6)	O(5)−Bi(7)−O(111)	110.2(7)	O(6)−Bi(7)−O(111)	121.2(7)
O(2)−Bi(2)−O(5)	73.0(7)	O(1)−Bi(2)−O(4)	72.1(6)	O(4)−Bi(7)−O(111)	64.7(7)	O(911)−Bi(7)−O(111)	163.4(7)
O(2)−Bi(2)−O(4)	125.6(6)	O(5)−Bi(2)−O(4)	70.5(6)	O(5)−Bi(8)−O(2)	73.5(7)	O(5)−Bi(8)−O(7)	90.2(7)
O(1)−Bi(2)−O(311)	97.8(8)	O(2)−Bi(2)−O(311)	61.5(7)	O(2)−Bi(8)−O(7)	73.3(7)	O(5)−Bi(8)−O(321)	86.1(7)
O(5)−Bi(2)−O(311)	125.3(7)	O(4)−Bi(2)−O(311)	163.0(7)	O(2)−Bi(8)−O(321)	69.1(7)	O(7)−Bi(8)−O(321)	141.7(7)
O(2)−Bi(3)−O(331)	77.1(8)	O(2)−Bi(3)−O(311)	68.8(7)	O(5)−Bi(8)−O(391)	140.3(7)	O(2)−Bi(8)−O(391)	68.6(7)
O(331)−Bi(3)−O(311)	87.8(10)	O(2)−Bi(3)−O(391)	71.9(7)	O(7)−Bi(8)−O(391)	90.1(6)	O(321)−Bi(8)−O(391)	69.8(7)
O(331)−Bi(3)−O(391)	82.2(8)	O(311)−Bi(3)−O(391)	140.7(7)	O(7)−Bi(9)−O(6)	95.9(7)	O(7)−Bi(9)−O(3)	74.5(7)
O(2)−Bi(3)−O(321)	67.4(7)	O(331)−Bi(3)−O(321)	139.6(7)	O(6)−Bi(9)−O(3)	74.2(7)	O(7)−Bi(9)−O(621)	128.6(7)
O(311)−Bi(3)−O(321)	96.6(9)	O(391)−Bi(3)−O(321)	69.1(7)	O(6)−Bi(9)−O(621)	100.9(6)	O(3)−Bi(9)−O(621)	64.3(6)
O(1)−Bi(4)−O(6)	94.6(6)	O(1)−Bi(4)−O(4)	75.2(6)	O(7)−Bi(9)−O(911)	75.6(7)	O(6)−Bi(9)−O(911)	70.4(7)
O(6)−Bi(4)−O(4)	71.8(6)	O(1)−Bi(4)−O(3)	69.1(6)	O(3)−Bi(9)−O(911)	130.3(7)	O(621)−Bi(9)−O(911)	155.6(6)
O(6)−Bi(4)−O(3)	67.7(6)	O(4)−Bi(4)−O(3)	122.3(6)	Bi(4)−O(1)−Bi(2)	113.2(7)	Bi(4)−O(1)−Bi(5)	116.3(7)
O(1)−Bi(4)−O(131)	83.8(6)	O(6)−Bi(4)−O(131)	133.4(7)	Bi(2)−O(1)−Bi(5)	116.6(7)	Bi(3)−O(2)−Bi(2)	120.1(9)
O(4)−Bi(4)−O(131)	62.8(6)	O(3)−Bi(4)−O(131)	148.1(6)	Bi(3)−O(2)−Bi(8)	107.3(8)	Bi(2)−O(2)−Bi(8)	106.1(8)
O(1)−Bi(4)−O(141)	134.9(6)	O(6)−Bi(4)−O(141)	81.7(6)	Bi(3)−O(2)−Bi(5)	117.5(8)	Bi(2)−O(2)−Bi(5)	101.7(7)
O(4)−Bi(4)−O(141)	60.9(6)	O(3)−Bi(4)−O(141)	143.7(6)	Bi(8)−O(2)−Bi(5)	102.2(7)	Bi(6)−O(3)−Bi(9)	117.8(8)
O(131)−Bi(4)−O(141)	68.1(7)	O(7)−Bi(5)−O(1)	93.0(7)	Bi(6)−O(3)−Bi(5)	108.9(8)	Bi(9)−O(3)−Bi(5)	102.3(7)
O(7)−Bi(5)−O(3)	72.2(7)	O(1)−Bi(5)−O(3)	71.9(6)	Bi(6)−O(3)−Bi(4)	119.8(8)	Bi(9)−O(3)−Bi(4)	103.3(7)
O(7)−Bi(5)−O(631)	79.8(7)	O(1)−Bi(5)−O(631)	134.2(6)	Bi(5)−O(3)−Bi(4)	102.6(7)	Bi(1)−O(4)−Bi(7)	119.1(8)
O(3)−Bi(5)−O(631)	62.8(7)	O(7)−Bi(5)−O(641)	134.4(6)	Bi(1)−O(4)−Bi(4)	110.3(7)	Bi(7)−O(4)−Bi(4)	104.8(7)
O(1)−Bi(5)−O(641)	83.3(6)	O(3)−Bi(5)−O(641)	63.5(6)	Bi(1)−O(4)−Bi(2)	119.8(7)	Bi(7)−O(4)−Bi(2)	100.7(6)
O(631)−Bi(5)−O(641)	71.5(7)	O(7)−Bi(5)−O(2)	68.9(7)	Bi(4)−O(4)−Bi(2)	99.4(6)	Bi(7)−O(5)−Bi(8)	125.9(8)
O(1)−Bi(5)−O(2)	67.5(6)	O(3)−Bi(5)−O(2)	120.8(6)	Bi(7)−O(5)−Bi(2)	112.6(8)	Bi(8)−O(5)−Bi(2)	107.2(7)
O(631)−Bi(5)−O(2)	143.5(7)	O(641)−Bi(5)−O(2)	144.8(6)	Bi(9)−O(6)−Bi(7)	120.2(8)	Bi(9)−O(6)−Bi(4)	114.7(8)
O(3)−Bi(6)−O(611)	76.9(8)	O(3)−Bi(6)−O(621)	69.1(7)	Bi(7)−O(6)−Bi(4)	109.9(7)	Bi(9)−O(7)−Bi(5)	110.4(8)
O(611)−Bi(6)−O(621)	88.2(8)	O(3)−Bi(6)−O(641)	69.0(7)	Bi(9)−O(7)−Bi(8)	125.5(9)	Bi(5)−O(7)−Bi(8)	114.6(8)
O(611)−Bi(6)−O(641)	82.5(7)	O(621)−Bi(6)−O(641)	138.1(7)				

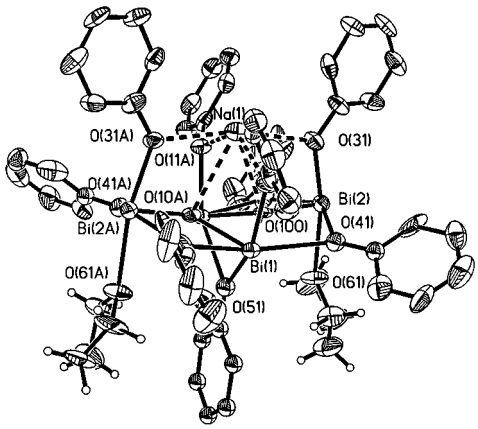

Figure 4. Thermal ellipsoid plot of **5**. The 30% probability level was chosen for clarity. Hydrogen and fluorine atoms have been omitted for clarity.

ROR.[10] In the solid state **8** exists as a chain polymer in which Na^+ and Bi^{3+} ions alternate, being connected by two μ-OR groups. Compound **9** possesses an oxide ligand situated in the center of an octahedron of positionally disordered metal ions having alkoxide ligands capping each of the faces of the octahedron. These compounds are structurally similar to ones reported by Schmidbaur and Veith.[23,24] In contrast to the reaction carried out in dichloromethane, dissolving **1** in chloroform yields **4** instead of **2**. As may be expected, dissolving **2** in chloroform results in its conversion to **4**.

Two possible reaction pathways are apparent for the formation of these products: ether elimination or hydrolysis. Although the reactions were carried out under rigorously dry conditions, hydrolysis cannot be ruled out completely and probably accounts for at least some of the oxide ligand production, since the presence of both pentafluorophenol (ROH; $\delta(CD_2Cl_2) = -162.1, -162.7, -167.4$ ppm; *m*/*e* 184) and bis(pentafluorophenyl) ether (ROR; *m*/*e* 350) was indicated by either NMR or GC/MS. The ether elimination has been established for the formation of the sodium bismuth oxo pentafluorophenoxides such as **5** and **8** by us,[10] and by Schmidbaur[24] in the case of related antimony compounds. In the case of $^tBuO^-$ complexes of antimony, elimination of 2-methyl-2-propene along with HO^t-Bu was found to be the mechanism by which oxide ligands were formed.[24] For our system, ROR always appears as a reaction product when Na^+ ions are found in the final product.

(23) Veith, M.; Yu, E.-C.; Hutsch, V. *Eur. J. Chem.* **1995**, *1*, 26.
(24) Baier, M.; Bissinger, P.; Blümel, J.; Schmidbaur, H. *Chem. Ber.* **1993**, *126*, 947.

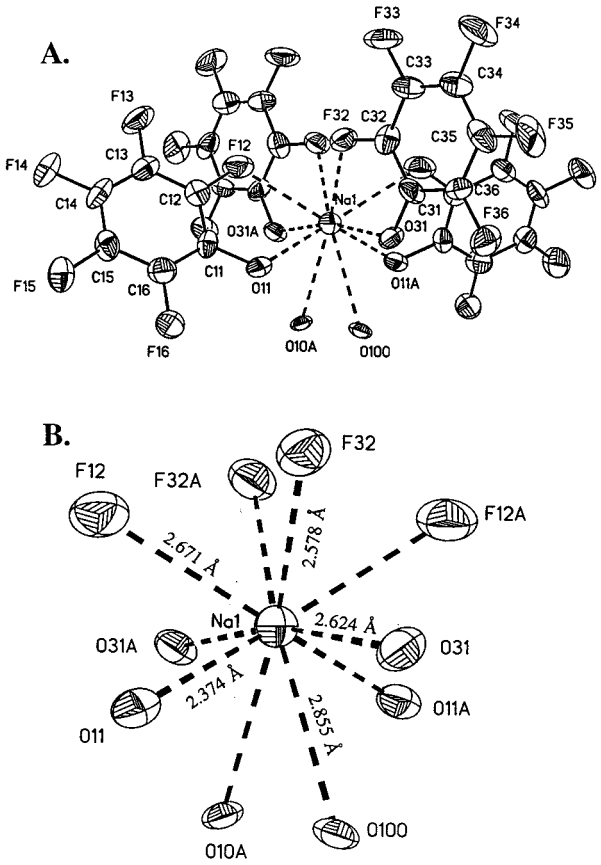

Figure 5. (A) Sodium ion coordination environment of **5** including the weakly interacting F atoms. (B) Sodium ion to oxide and fluoride ion distances of the plot given in (A).

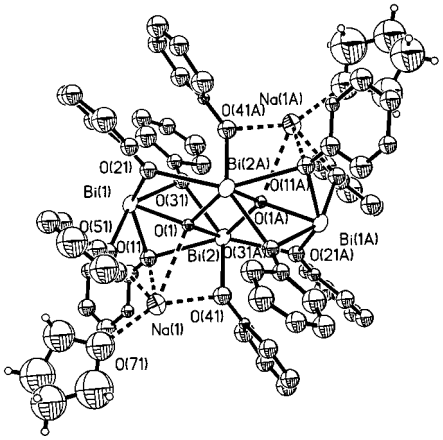

Figure 6. Thermal ellipsoid plot of **6** at the 50% probability level. Fluorine atoms have been omitted.

The thermodynamically most stable compound in this system appears to be complex **4**, which is synthesized in good yield by heating triphenylbismuth directly with pentafluorophenol in chloroform as well as by dissolving **1** or **2** in chloroform. When **1** was dissolved in CH_2Cl_2 (which has been shown to result in the formation of **2**) and then layered with 1-hexene, two types of crystals formed after the solution was allowed to stand at room temperature—pale yellow **3** and colorless **4**. Compound **3** was analyzed by X-ray diffraction only, because attempts to redissolve it in dichloromethane for spectroscopic analysis led to the formation of the more stable **4**. ^{19}F NMR signals of **3** were assigned by comparing the spectrum of **3** in CD_2Cl_2 with a spectrum of **4** in CD_2Cl_2. Several experiments were carried out to re-form **3** by controlling the amount of moisture or oxygen added to the system, but none were successful. The amount of compound **3** present in the products is highly variable, an observation that may be attributed to its instability with respect to **4**.

Formation of the Na^+ ion-containing **5** and **6** occurs using the salt metathesis methodology. Both ROH and ROR were present in the reaction solutions as confirmed by mass spectrometric analysis (see eqs 1−3). Compound **6** can be viewed as an NaOR adduct of **5**.

$$4BiCl_3 + 13NaOR \rightarrow 5 + 2ROR + 12NaCl \quad (1)$$

$$4BiCl_3 + 13NaOR + 2H_2O \rightarrow \mathbf{5} + 4ROH + 12NaCl \quad (2)$$

$$\mathbf{5} + NaOR \rightarrow \mathbf{6} \quad (3)$$

Structural Features of the Bismuth Oxo Alkoxides. Compounds **2**−**6** share two basic structural features which include the μ_3-OBi_3 unit (**10**) and the μ_4-OBi_4 unit (**11**). As noted earlier, the $(RO)_2BiOBi(OR)_2$ unit (**12**) is a formula subunit of a number of the compounds present in Scheme 1. For the larger clusters, the O-Bi$(OR)_4$ (**13**) unit may be found at the periphery of the central Bi_xO_y core. Invariably the OR groups in **13** show weak bridging tendencies toward the Bi atoms in the core. The composite unit shown as **14**, in which two Bi_3O units share an edge, is the basic unit from which **5** and **6** are made, but it is also observed as the central unit in **3** (see **15**). A variation of this is the inclusion of a μ_4-O atom (see **16**) as is found for **2**.

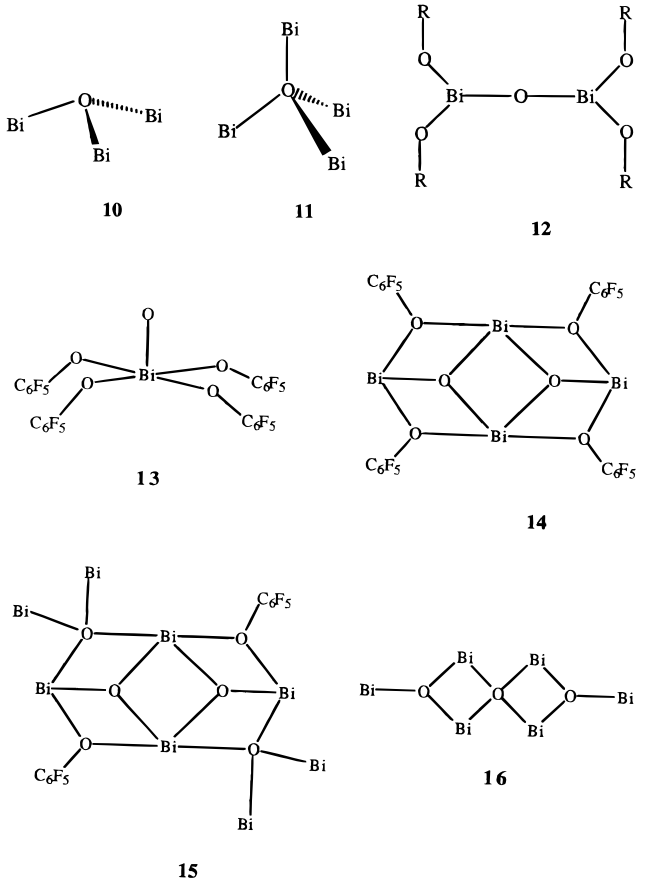

The geometries about these bridging oxo ligands are very similar in all compounds. The sum of the Bi-O-Bi angles around the μ_3-O atoms ranges from 338° to 357° as shown in Table 8. The oxo ligand O(2) of compound **3** has markedly pyramidal

Table 6. Selected Bond Lengths (Å) and Angles (deg) for **5**

			Distances				
Bi(1)−O(100)	2.189(9)	Bi(1)−O(100A)	2.193(10)	Bi(2)−O(21)	2.338(9)	Bi(2)−O(61)	2.532(11)
Bi(1)−O(11)	2.210(9)	Bi(1)−O(51)	2.421(18)	Na(1)−O(11)	2.374(10)	Na(1)−F(32)	2.578(11)
Bi(1)−O(51A)	2.504(18)	Bi(1)−O(21A)	2.519(10)	Na(1)−O(31)	2.624(9)	Na(1)−F(12)	2.671(10)
Bi(1)−O(41)	2.655(10)	Bi(2)−O(100)	2.042(10)	Na(1)−O(100)	2.855(12)		
Bi(2)−O(31)	2.188(9)	Bi(2)−O(41)	2.290(9)				
			Angles				
O(100)−Bi(1)−O(100A)	67.5(4)	O(100)−Bi(1)−O(11)	82.1(3)	O(11A)−Na(1)−O(31A)	83.0(3)	O(11)−Na(1)−O(31A)	91.6(3)
O(100A)−Bi(1)−O(11)	83.4(3)	O(100)−Bi(1)−O(51)	68.3(6)	F(32)−Na(1)−O(31A)	129.5(4)	O(31)−Na(1)−O(31A)	167.5(6)
O(100A)−Bi(1)−O(51)	73.1(6)	O(11)−Bi(1)−O(51)	147.4(5)	O(11)−Na(1)−F(12)	65.1(3)	O(11)−Na(1)−F(12A)	152.5(3)
O(100)−Bi(1)−O(51A)	71.5(6)	O(100A)−Bi(1)−O(51A)	66.7(6)	F(32A)−Na(1)−F(12A)	67.2(3)	F(32)−Na(1)−F(12A)	61.5(3)
O(11)−Bi(1)−O(51A)	145.7(5)	O(100)−Bi(1)−O(21A)	129.6(3)	O(31)−Na(1)−F(12A)	72.1(3)	O(31)−Na(1)−F(12)	115.1(3)
O(100A)−Bi(1)−O(21A)	63.8(3)	O(11)−Bi(1)−O(21A)	80.6(3)	F(32)−Na(1)−F(12)	67.2(3)	O(31A)−Na(1)−F(12)	72.1(3)
O(51)−Bi(1)−O(21A)	107.6(7)	O(51A)−Bi(1)−O(21A)	99.5(7)	F(12A)−Na(1)−F(12)	115.3(5)	O(11A)−Na(1)−O(100)	67.4(3)
O(100)−Bi(1)−O(41)	62.7(3)	O(100A)−Bi(1)−O(41)	129.4(3)	O(11)−Na(1)−O(100)	66.3(3)	F(32A)−Na(1)−O(100)	163.7(3)
O(11)−Bi(1)−O(41)	81.5(3)	O(51)−Bi(1)−O(41)	96.0(7)	F(32)−Na(1)−O(100)	120.1(3)	O(31)−Na(1)−O(100)	58.6(3)
O(51A)−Bi(1)−O(41)	104.2(7)	O(21A)−Bi(1)−O(41)	156.0(3)	O(31A)−Na(1)−O(100)	108.9(4)	F(12A)−Na(1)−O(100)	107.9(3)
O(100)−Bi(2)−O(31)	78.9(3)	O(100)−Bi(2)−O(41)	72.0(4)	F(12)−Na(1)−O(100)	131.4(3)	O(11)−Na(1)−O(100A)	67.4(3)
O(31)−Bi(2)−O(41)	94.4(4)	O(100)−Bi(2)−O(21)	69.4(4)	F(32)−Na(1)−O(100A)	163.7(3)	O(31)−Na(1)−O(100A)	108.9(4)
O(31)−Bi(2)−O(21)	99.0(4)	O(41)−Bi(2)−O(21)	135.4(3)	F(12)−Na(1)−O(100A)	107.9(3)	O(100)−Na(1)−O(100A)	50.5(4)
O(100)−Bi(2)−O(61)	87.6(4)	O(31)−Bi(2)−O(61)	166.2(4)	Bi(2)−O(100)−Bi(1)	126.1(5)	Bi(2)−O(100)−Bi(1A)	125.1(5)
O(41)−Bi(2)−O(61)	78.8(4)	O(21)−Bi(2)−O(61)	78.3(4)	Bi(1)−O(100)−Bi(1A)	103.0(4)	Bi(2)−O(100)−Na(1)	109.2(4)
O(11A)−Na(1)−O(11)	128.5(6)	O(11A)−Na(1)−F(32A)	97.0(3)	Bi(1)−O(100)−Na(1)	91.1(3)	Bi(1A)−O(100)−Na(1)	91.0(3)
O(11)−Na(1)−F(32A)	125.5(3)	F(32A)−Na(1)−F(32)	72.3(5)	C(11)−O(11)−Bi(1)	123.6(7)	C(11)−O(11)−Na(1)	122.5(8)
O(11A)−Na(1)−O(31)	91.6(3)	O(11)−Na(1)−O(31)	83.0(3)	Bi(1)−O(11)−Na(1)	104.7(4)		
F(32A)−Na(1)−O(31)	129.5(4)	F(32)−Na(1)−O(31)	62.6(3)				

[a] Symmetry transformations used to generate equivalent atoms: (A) $-x, y, -z + 1/2$.

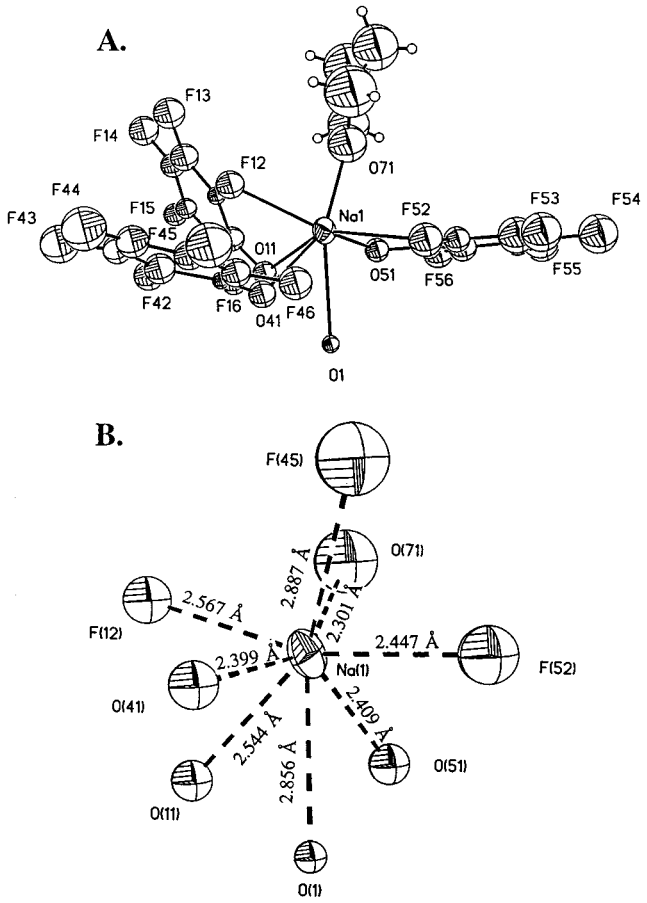

Figure 7. (A) Sodium ion coordination environment of **6** including the weakly interacting F atoms. (B) Sodium ion to oxide and fluoride ion distances of the plot given in A.

geometry when compared to all the other μ_3-O atoms of compounds **2**−**5**. The trigonal planar structure suggests some involvement of the oxygen lone pair of these atoms in their bonding to Bi. The Bi-O-Bi angles around the μ_4-O atoms connected to four bismuth atoms are very close to those expected for a tetrahedral geometry.

The central Bi_6O_3 core in **2** is surrounded by 12 bridging pentafluorophenoxide ligands (Figure 1). The overall formula of $Bi_6O_3(OR)_{12}$ is the same as the one with R = 2,6-$C_6H_3Cl_2$ published by James et al. (**17**),[25] but there is one noticeable

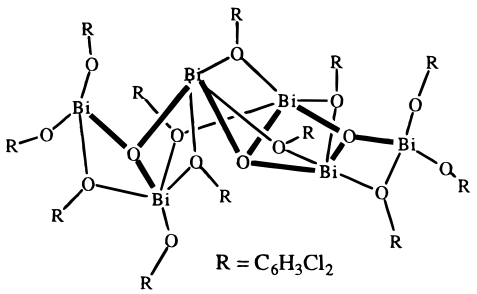

17

structural difference between those two compounds. The central oxide ligand does not adopt the μ_4-bridging mode seen as **2** but rather is only coordinated to three Bi atoms. This may likely reflect the increased steric requirements of the 2,6-$C_6H_3Cl_2$ group.

Bi(6) is coordinated to a THF solvent molecule, and Bi(1) is coordinated weakly to a toluene ring. The Bi(1) to toluene ring centroid distance is 3.073 Å, which is comparable to the distances found in the two reported forms of the dimer (2.968, 2.958 Å).[14] The ability of these compounds to coordinate and occlude solvent molecules in a variable fashion is a common but complicating feature in characterizing many of the compounds of this family.

Compound **3** (Figure 2) crystallizes with one molecule per unit cell which is situated about a crystallographic inversion center. The unique part of the molecule contains a Bi_4O tetrahedron, **11**, with one terminal and seven doubly bridging OR groups. The core structure is represented as **15**. It can also be viewed as two Bi_4O tetrahedral units connected via two μ_3-O ligands.

(25) James, S. C. N., N. C.; Orpen, A. G.; Quayle, M. J.; Weckenmann, U. *J. Chem. Soc., Dalton Trans.* **1996**, 4159.

Table 7. Selected Bond Lengths (Å) and Angles (deg) for **6**

Distances							
Bi(1)−O(1)	2.15(2)	Bi(1)−O(11)	2.32(2)	Bi(2)−O(31)	2.47(2)	Bi(2)−O(41)	2.20(2)
Bi(1)−O(21)	2.29(2)	Bi(1)−O(31)	2.46(2)	Na(1)−O(11)	2.53(3)	Na(1)−O(41)	2.40(3)
Bi(1)−O(51)	2.19(2)	Bi(2)−O(1)	2.17(2)	Na(1)−O(51)	2.41(3)	Na(1)−O(71)	2.30(3)
Bi(2A)−O(1)	2.20(2)	Bi(2)−O(21)	2.57(2)	Na(1)−F(12)	2.56(2)	Na(1)−F(52)	2.44(3)
Angles							
O(1)−Bi(1)−O(11)	70.1(8)	F(12)−Na(1)−F(52)	158.8(9)	O(1)−Bi(2)−O(21)	124.4(7)	O(11)−Na(1)−O(71)	112(1)
O(1)−Bi(1)−O(21)	70.3(7)	F(12)−Na(1)−O(11)	63.8(8)	O(1)−Bi(2)−O(31)	69.9(7)	O(41)−Na(1)−O(51)	128(1)
O(1)−Bi(1)−O(31)	70.3(7)	F(12)−Na(1)−O(41)	80.6(8)	O(1)−Bi(2)−O(41)	79.1(8)	O(41)−Na(1)−O(71)	148(1)
O(1)−Bi(1)−O(51)	82.3(8)	F(12)−Na(1)−O(51)	115.2(8)	O(1)−Bi(2)−O(21A)	64.3(7)	O(51)−Na(1)−O(71)	82(1)
O(11)−Bi(1)−O(21)	139.1(8)	F(12)−Na(1)−O(71)	76(1)	O(1)−Bi(2)−O(31A)	88.6(7)	O(1)−Bi(2)−O(41)	103.2(8)
O(11)−Bi(1)−O(31)	76.1(8)	F(52)−Na(1)−O(11)	132(1)	O(21)−Bi(2)−O(31)	137.6(7)	Bi(1)−O(1)−Bi(2)	109.5(8)
O(11)−Bi(1)−O(51)	78.0(8)	F(52)−Na(1)−O(41)	115.0(9)	O(21)−Bi(2)−O(41)	79.0(8)	Bi(1)−O(1)−Bi(2A)	119.4(9)
O(21)−Bi(1)−O(31)	100.1(7)	F(52)−Na(1)−O(51)	67.9(8)	O(31)−Bi(2)−O(41)	141.6(8)	Bi(2)−O(1)−Bi(2A)	108.0(8)
O(21)−Bi(1)−O(51)	86.7(8)	F(52)−Na(1)−O(71)	84(1)	Bi(1)−Na(1)−F(12)	102.2(6)	Bi(1)−O(11)−Na(1)	94.6(8)
O(31)−Bi(1)−O(51)	147.3(8)	O(11)−Na(1)−O(41)	75.1(8)	Bi(1)−O(21)−Bi(2)	101.0(8)	Bi(1)−O(31)−Bi(2)	91.4(8)
O(1)−Bi(2)−O(1A)	72.0(8)	O(11)−Na(1)−O(51)	70.1(8)	Bi(2)−O(41)−Na(1)	106(1)	Bi(1)−O(51)−Na(1)	102.0(9)

Scheme 1. Transformations of Various Bismuth Alkoxide and Oxo Alkoxide Compounds[a]

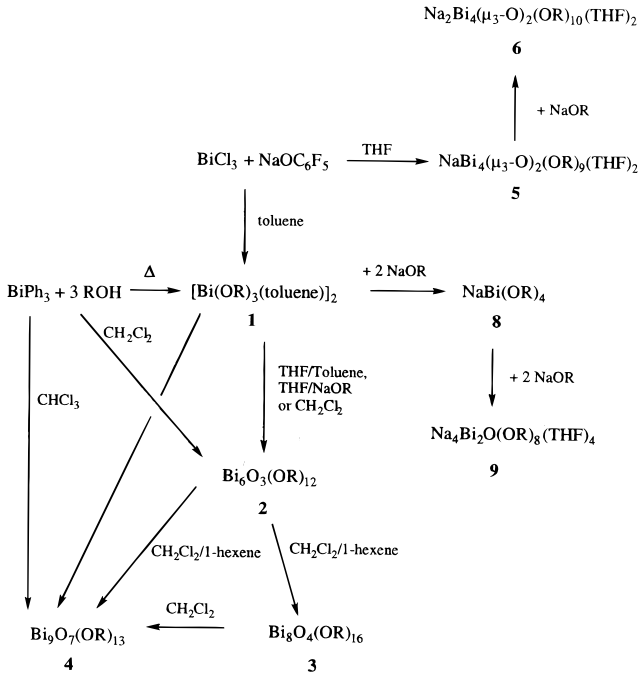

[a] Solvent molecules which may be ligated to the clusters have not been included in all cases for simplicity.

Figure 3 shows a schematic drawing of the largest bismuth oxo alkoxide complex yet known, **4**, which has been previously communicated[11] where six bismuth atoms and six oxygen atoms form two $(BiO)_3$ hexagons which are rotated with respect to each other by 60°. Three bismuth atoms in one plane are further bridged by a μ_3-OR, the three bismuth atoms in the second plane are bridged by a triply bridging oxygen (O(71)). Each of the three oxygen atoms in that second $(BiO)_3$ plane is bound to the bismuth of a $Bi(OR)_4$ group. Comparing **4** to **2** and **3** shows that it possesses the most compact metal oxide core, being very like what one would expect from a metal oxide particle. The central structure can be derived from close-packed layers of Bi atoms, with the oxide ions occupying tetrahedral holes.

These compounds and the sodium-containing complexes to be discussed shortly often show bismuth centers which may be thought to retain a "stereochemically active" lone pair of electrons. As with other bismuth coordination compounds, it is not clear why bismuth in some cases adopts configurations in which the lone pair appears to be stereochemically active and does not in others. This question is complex and requires first a discussion of what a stereochemically active lone pair is. Most often this is taken to be the situation in which a vacant coordination site is present on a *p*-block atom in which a lone pair of electrons is thought to reside. The situation almost always is used to refer to "hypervalent atoms", i.e., those which formally have greater than an octet of electrons around them. The term stereochemically active implies that the lone pair of electrons lies in an orbital that has directionality associated with it. However, for the heavier main group elements this may not entirely be the case. The related phenomenon which must also be accounted for is the inert pair effect, the empirical observation that the *s*-electrons are less available for bonding as one descends the periodic table. The result of the inert pair effect is that hybridization of the *s*- and *p*-orbitals becomes increasingly difficult. This was once explained very simplistically by arguing that the *s*-orbital electrons were "less available" for bonding, indicating that they were lower in energy and, therefore, more stable. However, a consideration of the ionization potentials indicates that this is not completely true. An alternate explanation is that the orbital overlap between the *s*-orbital for heavier *p*-block elements and the atoms to which they bond becomes less favorable as the *s*-orbital becomes larger and more diffuse. The result is that a vacant coordination site does not necessarily represent the location of a lone pair of electrons. For example, in a simple EX_3 compound where E is a group 15 element, the X−E−X bond angles tend to be closer to 90° than to the 109.5° commonly expected for tetrahedral sp^3 hybridization. The common explanation for this phenomenon is that it is primarily the *p*-orbitals which are involved in the bonding of the three X units to E. The result is that the lone pair of electrons is primarily in an *s*-type orbital which has spherical symmetry, regardless of the fact that the X groups would subtend X−E−X angles of ca. 90°. For hypervalent molecules, the situation is complicated by the mixing of the orbital of the additional donor lone pairs with the *s*-antibonding orbitals on the acceptor atom. Given that these molecules for the bismuth alkoxides are highly fluctional suggests that there is a very low energy barrier between structures which have a noticeable vacant coordination site and those that do not.

Structural Features of the Sodium Bismuth Oxo Alkoxides. The core of the structure of **5** is composed of two edge-sharing $Bi_3(\mu_3$-O) triangles with a crystallographic 2-fold axis passing through Na(1) (Figure 4). The μ_3-O atoms lie 0.24 Å above the Bi_3 planes pointing toward the Na atom (**18**) although the Na−O distance is long (Figure 5). All nine alkoxide ligands

Table 8. Sum of Bi−O−Bi Angles around μ_3-O Atoms (deg) for Compounds **2**−**6**

	2	3	4	5	6
∑∠Bi−O−Bi	O(1), 345.8 O(3), 345.1	O(2), 338.0	O(1), 346.1 O(5), 345.7 O(6), 344.0 O(7), 350.5	O(1), 355.1	O(1), 336.9

are doubly bridging between two metal atoms.

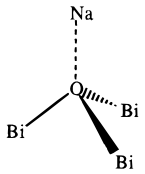

18

The coordination environment about Bi(1) is composed of six oxygen atoms and one lone pair of electrons in a distorted pentagonal bipyramidal array. Atoms O(40) and O(50) may be considered as the axial ligands, subtending an angle of 147.1(4)° at Bi(1). The angles between adjacent O atoms in the pentagonal plane range from 62.8(5)° to 66.5(5)°. The axial O atoms are clearly bent away from the location of the lone pair of electrons as are the two O atoms closest to the lone pair position (154.5(4)° vs 144° for a regular pentagon). These distortions agree with predictions made from simple VSEPR theory arguments.

The atoms Bi(2) and Bi(2a) are also symmetry related, and each binds three bridging alkoxides, one μ_3-oxide ligand, and one THF ligand. The arrangement around this bismuth atom is a distorted square pyramid. Variations in the O−Bi−O angles are consistent with those seen for Bi(1) above (∠O(20)−Bi(2)−O(30), 136.6(4)°; ∠O(10)−Bi(2)−O(200), 166.0(5)°). Similarly to that of compound **2**, the Bi−O(THF) distance is significantly longer than the Bi−O(alkoxide) values (2.498(13) Å vs 2.078(11)−2.367(12) Å). The sodium ion has four relatively short contacts to alkoxide oxygen atoms (Figure 5). Pseudooctahedral coordination is completed by two long contacts to fluorine atoms. In addition, the two μ_3-O ligands point toward the sodium ion but at longer distances.

Compound **6** is related to **5** in both formula and structure. Compound **6**, which sits on a crystallographic inversion center, can be viewed as the product of the addition of NaOR to **5**. A curiousity of the structure is that the THF ligands in **5** are bound to Bi while in **6** they are bound to Na. In both molecules the metal oxo core is composed of two edge-sharing triangles of bismuth atoms having μ_3-O ligands capping both triangles. They differ in that the μ_3-oxide ligands lie on the same side of the Bi_4 unit in **5** but on opposite sides in **6**. This is attributable to the presence of the Na^+ ions. In **5**, there is only one Na^+ ion, and both oxide ligands are oriented toward that ion (**19**), while in **6**, there are two Na^+ ions that lie on opposite sides of the Bi_4 unit and act as a directing influence for the positioning of the μ_3-O ligands (**20**). As in **5**, there are two short Na···F

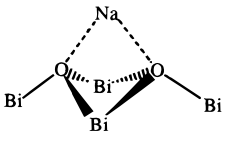

19

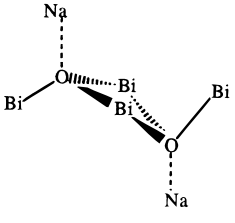

20

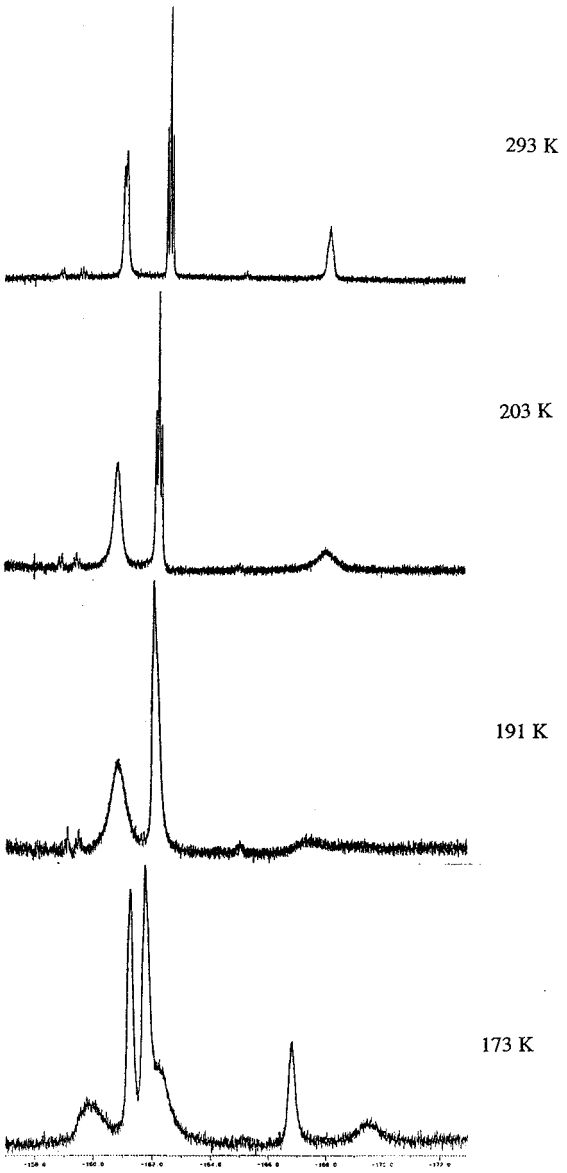

Figure 8. ^{19}F VT NMR of compound **4** in d_8-toluene.

contacts. Again the Na^+ ion sits in a very distorted octahedral cavity created by four oxygen atoms and two fluorine atoms of alkoxide ligands (Figure 7). Additionally the μ_3-O is directed toward the Na^+ ion at a much greater distance than in **5**. In both **5** and **6**, it may be better to consider the Na^+ ions sitting in roughly spherical cavities of negative charge created by the envelope of O and F atoms rather than as adopting a specific coordination geometry.

Solution Dynamics. Variable-temperature (VT) ^{19}F NMR was carried out to determine the structure of **4** in solution (Figure 8). As expected, at room temperature the exchange of the OR groups with each other is fast on the NMR time scale; we observe one set of three peaks with the ratio 1:2:2 = *para*:*meta*:*ortho*. Upon cooling, the peaks broaden; between $T = 191$ K and $T = 196$ K the *p*-fluorine peak has reached coalescence and splits into two peaks when the temperature is lowered

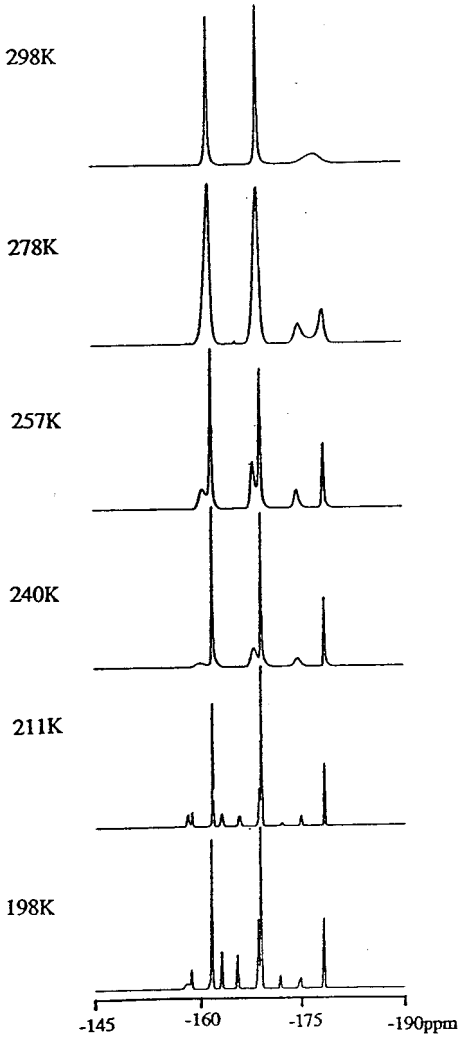

Figure 9. ^{19}F VT NMR of compound **5** in d_6-acetone.

further. Also the *m*- and *o*-fluorine atoms have now split into two environments. The slowing of the rotation about the O−Bi-(OR)$_4$ bond is a possible explanation for this phenomenon. There is no visible set of signals for the μ_3-OR probably due to rapid exchange with the other 12 phenoxide ligands. The sample froze at 173 K, without showing any additional changes in the NMR spectrum. Attempts to record a VT NMR spectrum of pure **2** failed, because traces of **4** formed in d_8-toluene, d_6-acetone, and CD_2Cl_2 solutions of **2** after 20 min. Hence, the VT NMR spectrum for **2** corresponds to a mixture of **2** and **4**. The peaks of **4** in the mixture were assigned by comparison to the spectra of pure **4**, with the remaining peaks assigned to **2** as listed in Table 1. It was not possible to slow the exchange mechanism of the pentafluorophenoxide groups enough to completely resolve the NMR signals.

In the solid state, the nine pentafluorophenyl rings of molecule **5** exist in five unique environments (one ring located near the 2-fold axis and four sets of two related by the C_2 axis). In solution it is assumed that the μ-oxo−bismuth bonds are stable and hold the bismuth core together, with the OR groups being fluxional and exchanging intramolecularly. If all OR ligands exchange in solution, a single environment would be observed, as is clearly the case (Figure 9). The ratio of the three peaks is 2:2:1, as expected for a single OR group. As the temperature is cooled to 278 K, the *ortho* and *meta* position signals broaden but do not resolve. The *para* peak, however, splits into two equal-intensity, broad signals. The peaks remain

Scheme 2

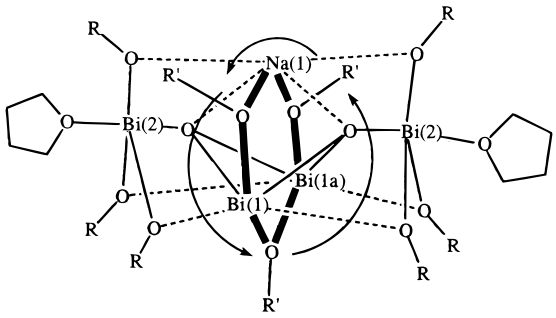

in a ratio of 2:2:1 if the areas of the two *para* peaks are combined.

As the temperature is lowered to 257 K, peaks 1 and 2 show unresolved splitting, but for the *p*-fluorine atoms two distinct environments become evident in a 3:6 ratio. The OR ligands attached to Bi(2) and Bi(2a) are equivalent if the bridging linkages to the Bi(1) and Bi(1a) atoms are broken and the alkoxides allowed to rotate about Bi(2)/Bi(2a) atoms. The remaining three alkoxide ligands which are bridging between Bi(1) and Bi(1a) as well as between Na(1) and Bi(1)/Bi(1a) (OR′ and OR″, Scheme 2) can be envisioned to migrate via bridge−terminal interconversions around the edges of the Bi-(1)−Na(1)−Bi(1a) triangle.

As the temperature is lowered to 240 K, the second environment begins to broaden, while that representing six rings sharpens further. The ratio of these two environments remains the same, and the peaks do not shift significantly. By the time the temperature has reached 220 K, however, the environment due to three equivalent phenyl rings has broadened, coalesced, and split into two environments with a ratio of 2:1. This now gives an overall ratio of 6:2:1 for three different R groups. The chemical shift of the six equal phenyl rings has remained essentially the same, but the component peaks (*ortho*, *meta* and *para*) have sharpened, and coupling starts to resolve. The migration of the three rings around the bismuth and sodium triangle is now slow relative to the NMR time scale at this temperature, causing the peak to split into two environments. One ring is now fixed, bridging between the two symmetry-equivalent bismuth atoms Bi(1) and Bi(1a), and the other two each bridge between the sodium and bismuth atoms.

At 211 K, three environments are clearly visible in a ratio of 1:2:6 for the *para* peak and 2:4:12 for peak 1. These are only partially resolved for peak 2 with the ratio 2:(4 + 12). At 198 K the same three environments were still clearly present. The sample froze at 195 K, preventing further study at lower temperatures.

Conclusions

The formation of soluble, larger polymetallic bismuth oxo alkoxides **2**, **3**, and **4** is accomplished by dissolving dinuclear **1** in different solvents. The degree of oligomerization is influenced by the type of solvent used and may result from the limit of residual water present after the solvent purification. The more polar solvent chloroform leads to the formation of the larger oxo alkoxide **4**. Using less polar solvents, toluene/THF or dichloromethane, the smaller oxo alkoxides **2** and **3** are formed. Therefore, the choice of solvent gives control over the degree of oligomerization, which will allow for some control over the bismuth to oxide ion ratio in the alkoxide. In those oligomerization reactions ether elimination or microhydrolysis can be the driving force for the oxo ligand formation. Reactions

involving the reagent NaOR have a strong tendency to produce products retaining Na^+ ions and possessing oxide ligands generated upon the elimination of the ether ROR. In cases were sodium ions are present in the final product, the pathway appears to proceed predominantly via ether elimination, whereas routes to non-sodium-containing species results in the formation of bis(pentafluorophenyl) ether as well as pentafluorophenol. Oxide ion formation can be avoided by conducting the synthesis in nonpolar toluene as illustrated for synthesis of **1** by reaction of NaOR with $BiCl_3$ in toluene rather than THF. This method is also viable for the production of $Bi(OC_6Cl_5)_3$.

In the solid-state structures, the bismuth atoms strongly prefer hypervalent structures—structures which exceed the octet rule by one, two, or even three electron pairs. This tendency is enhanced by the electron-withdrawing fluorinated alkoxide ligands. The molecules are highly Lewis acidic, resulting in the coordination of donor solvent molecules to the bismuth atoms. This extends to the coordination of unsaturated aromatic hydrocarbons. We conjecture that binding of other unsaturated substrates such as olefins and dienes may be possible and would be relevant to the commercial oxidation or ammoxidation of propene. Because of the numerous modes of solvation, there is a strong tendency to form a wide variety of crystal morphologies corresponding to different solvations of the same fundamental compound. While the bismuth oxo cores of the solid compounds appear to be retained in solution, the alkoxide ligands are extremely fluxional, presumably intramolecularly, at room temperature and in some cases even to −95 °C.

Acknowledgment. The support of this research by the Robert A. Welch Foundation and the Petroleum Research Fund is gratefully acknowledged. We are also indebted to one reviewer for pointing out the relationship of the compound stoichiometries to the hypothetical $Bi_2O(OR)_4$ unit.

Supporting Information Available: Five X-ray crystallographic files in CIF format and figures with the complete atom labeling scheme for compounds **2**−**6**. This material is available free of charge via the Internet at http://pubs.acs.org.

IC990431M